

A Polynomial Approach to the Spectrum of Dirac-Weyl Polygonal Billiards

M. F. C. Martins Quintela* and J. M. B. Lopes dos Santos

3rd August 2020

Centro de Física das Universidades do Minho e do Porto, CF-UM-UP e Departamento de Física e Astronomia, Universidade do Porto, Rua do Campo Alegre 4169-007, Porto, Portugal.

The Schrödinger equation in a square or rectangle with hard walls is solved in every introductory quantum mechanics course. Solutions for other polygonal enclosures only exist in a very restricted class of polygons, and are all based on a result obtained by Lamé in 1852. Any enclosure can, of course, be addressed by finite element methods for partial differential equations. In this paper, we present a variational method to approximate the low-energy spectrum and wave-functions for arbitrary convex polygonal enclosures, developed initially for the study of vibrational modes of plates. In view of the recent interest in the spectrum of quantum dots of two dimensional materials, described by effective models with massless electrons, we extend the method to the Dirac-Weyl equation for a spin-1/2 fermion confined in a quantum billiard of polygonal shape, with different types of boundary conditions. We illustrate the method's convergence in cases where the spectrum is known exactly and apply it to cases where no exact solution exists.

1 Introduction

One of the first problems solved in introductory quantum mechanics courses is that of particle enclosed in a square or rectangular box with hard walls—Dirichlet boundary conditions, $\psi(\mathbf{r}) = 0$ at the boundary. Separation of variables easily turns the problem into two one-dimensional problems and the solutions are a finite sum of plane waves. The circle and the ellipse are also amenable to an exact treatment, again with separation of variables. But the vast majority of students are never led to consider the case of general polygonal enclosures.

*mfcmquintela@fc.up.pt

The eigenvalue problem of the Schrödinger equation for an equilateral triangle with hard boundaries was solved, long before Schrödinger’s equation even came into existence, by Lamé [1] in 1852. This solution has been revisited often from different perspectives [2, 3, 4, 5, 6]. As in the case of a rectangle, Lamé’s solution is also a finite sum of plane waves, built to satisfy the boundary conditions, and remarkably, it has even been proven that the only shapes that share this feature are the square, the rectangle, the equilateral triangle, the half-square (right isosceles triangle) and the half equilateral triangle (30-60° triangle) [7].

Following the pioneering work of Berry and Mondragon [8], and the discovery that two-dimensional (2D) materials, such as graphene, can be described by effective continuum models with the Dirac-Weyl equation [9, 10], there has been a upsurge of interest in the properties of confined relativistic particles (Dirac Billiards), either because low energy solutions have possible relevance for quantum dots of 2D materials [11, 12, 13, 14], or to address fundamental questions concerning the classical-quantum relations and energy-level statistics in the semi-classical limit [15, 16, 17, 8].

Lacking exact analytical solutions, one usually has to resort to numerical methods, and finite element methods of integration of partial differential equations have universal application [13]. But such methods give little physical insight into the solutions. The aim of this article is to present an essentially variational method that can yield the low energy spectrum of convex polygonal enclosures, both in the Schrödinger and Dirac equation cases, with the added benefit of providing approximate wave-functions which are polynomials. The method is well known in the Mechanical Engineering literature, in the context of the Helmholtz equation [18, 19, 20], where it was developed for the study of vibration of polygonal plates. The extension to the Schrödinger equation for free particle is trivial—the eigenvalue problem is the same as the Helmholtz problem—, but, to our knowledge, its extension to the Dirac-Weyl equation has not been presented before.

This paper is structured as follows. In section 2, we present the polynomial method for the simple case of the Schrödinger equation, more specifically for the textbook problem of the particle confined to a square well, and assess the convergence of the spectrum against the exact solution for this problem. We then apply the method to an hexagonal enclosure, a problem that has no analytical solution.

Section 3 reviews the different types of boundary conditions (BC) for the Dirac-Weyl equation, following closely reference [8]. We extend the polynomial method to 2-component spinors and the different types of BC, and illustrate it in exactly solvable one-dimensional enclosures. In sections 3.3–3.5 we study three different 2D polygonal enclosures with this method, the circle, the square and the hexagon. For a specific boundary condition, the solution of the former can be obtained from the solution of Lamé [1], and we compare our numerical results with the analytical ones [14].

2 The Polynomial Method for convex polygonal enclosures

2.1 The method: general idea

The essential idea of the polynomial method [18, 19, 20] is to generate orthonormal polynomials of increasing order that satisfy, from the start, the required boundary conditions (BC). In the Oxy

plane a linear polynomial in x and y , $\mathcal{P}_1(x, y) = a_0 + a_1x + a_2y$ will be zero in a straight line, $a_0 + a_1x + a_2y = 0$. It follows that a product of n such polynomials trivially satisfies the condition $\mathcal{P}_n(x, y) = 0$ at the boundary of a polygonal convex region. After normalization, such a function is a zero-th order approximation to the ground state.

As an example, for a right triangle with vertexes $(0, 0)$, $(1, 0)$, $(0, 1)$ we would choose

$$\psi_0(x, y) = N_0xy(1 - x - y) \quad (1)$$

with

$$\begin{aligned} N_0 &= \left[\int_0^1 dx \int_0^{1-x} dy [xy(1 - x - y)]^2 \right]^{-1/2} \\ &= 12\sqrt{35} \end{aligned}$$

If we multiply $\psi_0(x, y)$ by any polynomial, $\psi(x, y) = \mathcal{P}(x, y)\psi_0(x, y)$, we end up with a function that still satisfies the BC. We therefore proceed to generate a set of linearly independent functions

$$\psi_n(x, y) = \mathcal{P}_n(x, y)\psi_0(x, y) \quad (2)$$

where $\{\mathcal{P}_n(x, y) : n = 0, 1, \dots\}$ is a family of ascending-order monomials/polynomials. These can be generated by taking into account the symmetries of the enclosure in question, as a simple ordering of monomials, or as a generalization of Legendre polynomials discussed by Larcher [21]. In [20] the authors resort to the sorting

$$\{1, x, y, xy, x^2, y^2, x^2y, y^2x, x^2y^2, x^3, \dots\}. \quad (3)$$

We truncate the series at a finite n and orthonormalize the functions, typically through Gram-Schmidt orthogonalization. The Hamiltonian matrix in this truncated basis is calculated and diagonalized. For regular polygons, one can take into account the symmetry group of the enclosure by replacing the monomials of Eq.(3) by increasing order polynomials that transform according to irreducible representations of the symmetry group [22]. The Hamiltonian matrix becomes block diagonal, and the resulting eigenstates end up classified according to their symmetry properties.

The problem of the Schrödinger equation for a particle confined to a square well, provides a suitable example to assess convergence.

2.2 The square well: convergence

The exact spectrum of the Schrödinger equation for a particle confined to a square well is

$$E_{n_1, n_2} = \frac{\hbar^2 \pi^2}{2m L^2} (n_1^2 + n_2^2), \quad (4)$$

where L is the side length of the enclosure, and $n_{1(2)}$ positive integers.

Centering the enclosure at the origin, the starting wavefunction is

$$\psi_0(x, y) = N_0 \left[\left(\frac{L}{2} \right)^2 - x^2 \right] \left[\left(\frac{L}{2} \right)^2 - y^2 \right]. \quad (5)$$

The higher order basis functions are generated as described previously, by multiplication by $x^m y^n$ monomials. Both the orthogonalization and the calculation of the matrix elements of the kinetic energy operator reduce to the calculation of integrals of $x^m y^n$ monomials in the domain of the enclosure; these are easily calculated symbolically and stored. Keeping the computation symbolic up until the diagonalization of the Hamiltonian avoids stability problems of the Gram-Schmidt procedure. We computed the Hamiltonian matrix for different basis sizes, and diagonalized it numerically using standard packages. The results are shown in Fig.1, overlaid with the exact eigenvalues.

The method is seen to converge towards the exact eigenvalues as we increase the basis size. As the index of the eigenvalue increases, we require a larger basis, as expected. The numerical results indicate, roughly, that to get the lowest n eigenvalues to within 1% accuracy requires of the order of $3n$ basis functions.

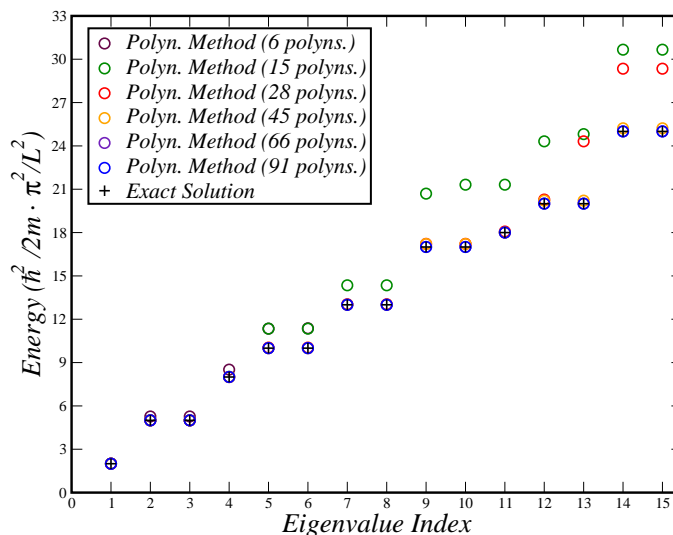


Figure 1: Convergence of the eigenvalues of the Hamiltonian in a square enclosure (polynomial method versus exact solution).

2.3 The hexagonal enclosure

To apply this procedure to the Schrödinger equation for a particle confined to an hexagonal well of side length L , we define the initial normalized polynomial as

$$\begin{aligned} \psi_0(x, y) = N_0 & \left(\frac{3L^2}{4} - y^2 \right) \left[L^2 - \left(x - \frac{y}{\sqrt{3}} \right)^2 \right] \\ & \times \left[L^2 - \left(x + \frac{y}{\sqrt{3}} \right)^2 \right]. \end{aligned} \quad (6)$$

We again calculated the Hamiltonian matrix elements for different basis sizes, and diagonalized it numerically using standard packages. The results are shown in Fig.2, overlaid with the eigenvalues obtained via direct numerical integration of the partial differential equation (PDE), by finite elements method. The convergence is similar to the one found in the case of the square.

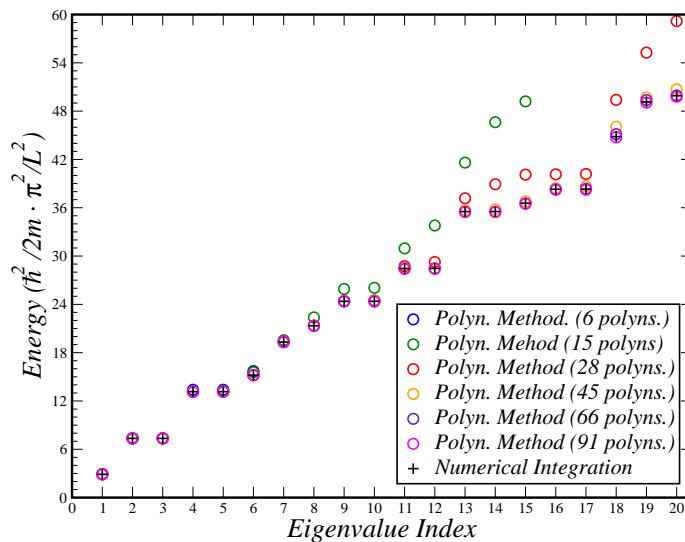


Figure 2: Convergence of the eigenvalues of the Hamiltonian in an hexagonal enclosure (polynomial method versus direct numerical integration of PDE).

As an illustration of this method, we applied it to different polygons with increasing number of sides and plot the lowest eigenvalues against the inverse number of sides (squared) in Fig.3, where the result for the circle, ϵ_i^∞ , $i = 1, 2, 3$, is the analytical solution.

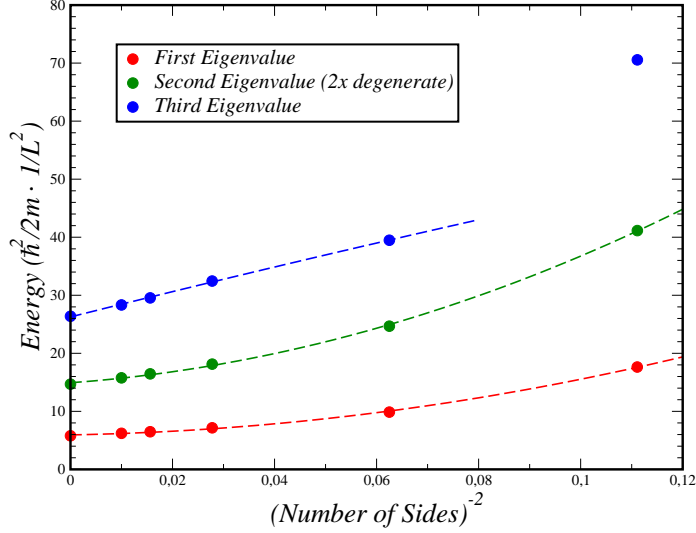


Figure 3: Comparison of the first three distinct energy levels as a function of the inverse of the number of sides of the polygon squared.

The dashed lines are fits of the form $\epsilon_i(n) = \epsilon_i^\infty + a_2 n^{-2} + a_4 n^{-4}$, where n is the number of sides. A suitable fit could not be found for the third eigenvalue, and the point for $n = 3$ was excluded. The remaining data points are well fitted with $a_4 = 0$.

We now turn to the extension of these results to the Dirac-Weyl equation.

3 Confinement of Dirac–Weyl electrons

3.1 Boundary Conditions in Neutrino Billiards

Berry and Mondragon [8] were the first to address the issue of the boundary conditions of a two-component spinor solution of the Dirac-Weyl equation in a confining planar enclosure. The eigenvalue equation is

$$-i\hbar v_F \boldsymbol{\sigma} \cdot \nabla \Psi = E \Psi. \quad (7)$$

where $\boldsymbol{\sigma} = (\sigma_x, \sigma_y)$. We assume a confining boundary at $y = 0$, excluding the region $y < 0$. The probability current is given by

$$\mathbf{j} = v_F \Psi^\dagger \boldsymbol{\sigma} \Psi = v_F \langle \boldsymbol{\sigma} \rangle, \quad (8)$$

which means that a necessary condition for confined states is

$$\langle \sigma^y \rangle_{\text{boundary}} = 0. \quad (9)$$

This condition implies that the spinor at the boundary must be an eigenstate of $\sigma_u = \boldsymbol{\sigma} \cdot \mathbf{u}$, where $\mathbf{u} = \cos \theta \mathbf{e}_z + \sin \theta \mathbf{e}_x$. *i.e.*,

$$\begin{bmatrix} \cos \theta & \sin \theta \\ \sin \theta & -\cos \theta \end{bmatrix} \begin{bmatrix} \psi_A \\ \psi_B \end{bmatrix} = \eta \begin{bmatrix} \psi_A \\ \psi_B \end{bmatrix}, \quad \eta = \pm 1, \quad (10)$$

or simply

$$\frac{\psi_B}{\psi_A} = \frac{\eta - \cos \theta}{\sin \theta}. \quad (11)$$

Denoting $t := \tan(\theta/2)$, simple trigonometric identities lead us to

$$\frac{\psi_B}{\psi_A} = t, \quad (12)$$

with a spinor, at the boundary, given by

$$\begin{bmatrix} \psi_A \\ \psi_B \end{bmatrix} = \frac{1}{\sqrt{1+t^2}} \begin{bmatrix} 1 \\ t \end{bmatrix} \quad (13)$$

for $\eta = +1$. The case for $\eta = -1$ is obtained by the substitution $t \rightarrow -1/t$, or by changing $\theta \rightarrow \pi - \theta$. As such, this is not a different solution, and we keep only $\eta = +1$.

Some special cases are:

- $t = 0$ or $t \rightarrow \infty$ (Dirichlet boundaries)

$$\begin{cases} t = 0, & \psi_B = 0; \\ t \rightarrow \infty, & \psi_A = 0 \end{cases}; \quad (14)$$

so that, at the boundary, $\langle \sigma^z \rangle = \pm 1$.

- $t = \pm 1$

$$\psi_A = \pm \psi_B. \quad (15)$$

In this case, the spin points along the x -direction.

The latter case corresponds to the infinite-mass confinement by Berry and Mondragon [8]. They considered adding a spatially dependent mass (gap) term,

$$-i\hbar v_F \boldsymbol{\sigma} \cdot \nabla \Psi + m(\mathbf{r}) \sigma_z = E \Psi. \quad (16)$$

and showed that continuity of the spinor components at the boundary, with $m(\mathbf{r}) = 0$ inside the enclosure, and $m(\mathbf{r}) \rightarrow \infty$ outside, leads to BC of the type of Eq.(15). Similarly, one can show that a mass term of the form [22]

$$m(\mathbf{r}) (\sigma^z - \cos \theta) \quad (17)$$

leads to the more general BC of Eq.(12) with $t = \tan(\theta/2)$. The cases $t = 0$ or $t \rightarrow \pm\infty$ correspond to Dirichlet boundaries in one of the spinor components, as in the case of zigzag boundaries in graphene.

If the boundary is at an angle ϕ with the x -axis, one must rotate the spinor in Eq. 13, resulting finally in

$$\Psi = \frac{e^{-i\phi\sigma_z/2}}{\sqrt{1+t^2}} \begin{bmatrix} 1 \\ t \end{bmatrix} = \frac{1}{\sqrt{1+t^2}} \begin{bmatrix} e^{-i\phi/2} \\ e^{i\phi/2}t \end{bmatrix}. \quad (18)$$

We will now show how to extend the polynomial method defined in Section 2 to this new type of BC. As an illustration we begin with 1D cases, where one easily computes the exact spectrum.

3.2 One-Dimensional Dirac-Weyl confinement

Consider the simple case where $t = 1$ and the confined region is the interval $y \in [-L/2, L/2]$. The BC are $\psi_B(-L/2)/\psi_A(-L/2) = 1$ at one end, and $\psi_B(L/2)/\psi_A(L/2) = -1$, at the other ($\phi = \pi$ in Eq.(18)). Measuring energies in units of $\hbar v_F/L$, $\epsilon = E/(\hbar v_F/L)$,

$$\begin{aligned} -\partial_y \psi_B &= \epsilon \psi_A \\ \partial_y \psi_A &= \epsilon \psi_B \end{aligned} \quad (19)$$

Squaring the Hamiltonian, one sees that the solutions have the form

$$\begin{aligned} \psi_B &= f_1 e^{iqy} + f_2 e^{-iqy} \\ \psi_A &= f_3 e^{iqy} + f_4 e^{-iqy}, \end{aligned} \quad (20)$$

with $\epsilon = sq$, $s = \pm 1$. With no loss of generality we assume $q > 0$. The Dirac-Weyl equation implies

$$\begin{aligned} f_4 &= isf_2 \\ f_3 &= -isf_1 \end{aligned}$$

The BC then imply

$$\begin{aligned} (1 - ist) f_1 + (1 + ist) f_2 e^{-iqL} &= 0 \\ (1 + ist) f_1 + (1 - ist) f_2 e^{iqL} &= 0 \end{aligned} \quad (21)$$

A non-zero solution to this homogeneous system of 2 equations, for $t = 1$, requires

$$(1 - is)^2 e^{iqL} = (1 + is)^2 e^{-iqL} \quad (22)$$

or

$$q = \frac{\pi}{2L} (2n + 1) \quad (23)$$

and the energies are

$$\epsilon_s(n) = s \hbar v_F \frac{\pi}{2L} (2n + 1) \quad n \geq 0, s = \pm 1 \quad (24)$$

The Dirac-Weyl equation in free space has electron-hole symmetry; it is easily seen that for any solution $\Psi = [\psi_A, \psi_B]^T$ of energy E , the state $\bar{\Psi} = [\psi_A, -\psi_B]^T$ is a solution of energy $-E$. But the BC we are choosing, $\psi_B/\psi_A = \pm 1$, breaks this symmetry, because Ψ and $\bar{\Psi}$ cannot both obey these BC. This can be traced to the mass term we introduced outside the confining region to derive the BC: it explicitly breaks this particle-hole symmetry. Nevertheless, the spectrum of eigenvalues remains symmetrical (Eq.24), because it is still true for this complete 1D Hamiltonian, inside and outside the enclosure, that σ_x is a chiral symmetry operator, $\sigma_x \hat{H} \sigma_x = -\hat{H}$.

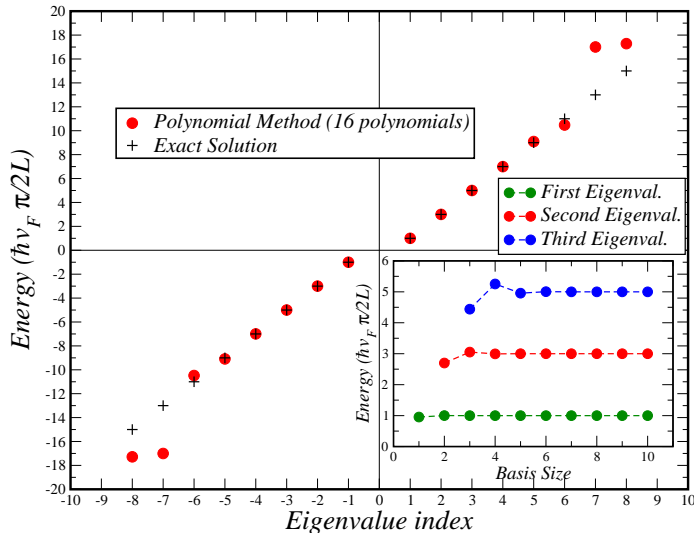


Figure 4: Exact solution vs polynomial approximation for a 1-D strip with $t = 1$. Convergence of the first three eigenvalues in the inset.

To implement the polynomial method, we must first realize that the parities of ψ_A and ψ_B are opposite. We therefore choose for the spinor components as the lowest order polynomials that satisfy the BC. For the conduction band ($s = 1$) we have,

$$\Psi_0^{(1)} = N_0 \begin{bmatrix} 1 \\ -\frac{y}{L/2} \end{bmatrix} \quad (25)$$

where N_0 is a normalization constant. To obtain the valence band solution, $s = -1$, it is enough to swap $\psi_A \leftrightarrow \psi_B$. The basis is now generated by functions of the form $\Psi_n^{(s)} = \mathcal{P}_n(y) \Psi_0^{(s)}$, orthonormalized by the Gram-Schmidt process. One must take care, however, to orthogonalize states between the valence and conduction bands, as the states generated this way for $s = 1$ and $s = -1$ are not orthogonal to start with.

Having generated the basis, one easily computes and diagonalizes the Hamiltonian matrix. We obtained the approximate spectrum visible in Fig.4; the inset shows the convergence analysis of the first three eigenvalue of the conduction band. An almost exact match is also present in the first

eigenfunction of the conduction band, as shown in Fig.5.

Having checked the validity of this method against a simple solution of the Dirac-Weyl equation, we will now proceed to consider planar enclosures.

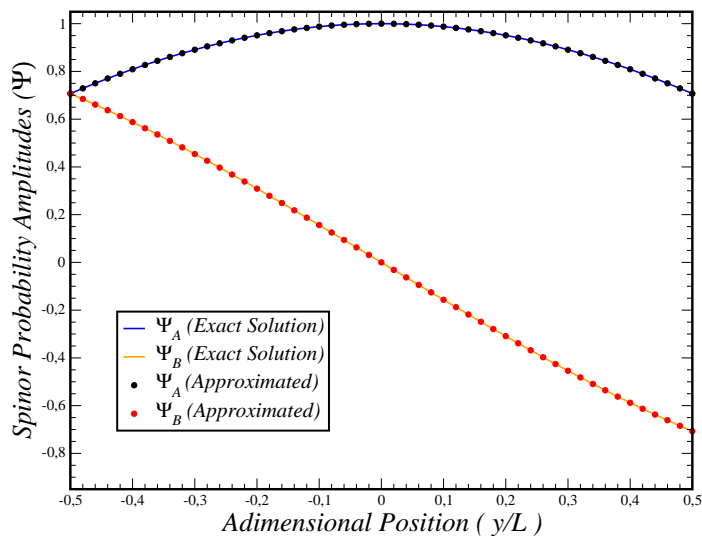


Figure 5: Comparison between the exact solution (full lines) and the lowest-energy polynomial eigenfunction (dots) for 16 polynomials.

3.3 Two-Dimensional Enclosures

To generalize this procedure to two-dimensional enclosures, we must be aware of a difference between Dirichlet boundaries and boundaries with finite t . If one has a Dirichlet BC, one can square the Dirac-Weyl Hamiltonian and easily prove that each spinor component obeys a Schrödinger equation inside the enclosure where the mass term is zero. As such, one can use the method we presented before for this equation to calculate the square of the eigenvalues and the spinor component that is zero at the boundary. Since the Dirac-Weyl equation has particle-hole symmetry—if one changes the sign of one of the spinor components in a state with energy E , one obtains a state of energy $-E$, which still preserves the Dirichlet BC—, one effectively obtains all the eigenvalues. Applying the Dirac operator to the component which is zero at the Boundary, one generates the other component of the spinor and completes the solution [14].

3.3.1 Non-Dirichlet Boundary Conditions

The same procedure cannot be used for finite t , when the BC only fixes the *ratio* between the spinor components, $\psi_B/\psi_A = te^{i\phi}$. The circle is the only 2D enclosure where an exact solution is known

for the infinite-mass BC we are using [22]. The solution is given by [23]

$$\Psi_{\epsilon,m}(r,\theta) = \begin{bmatrix} e^{im\theta} \mathcal{J}_m(q_\epsilon r) \\ is e^{i(m+1)\theta} \mathcal{J}_{m+1}(q_\epsilon r) \end{bmatrix} \quad (26)$$

where $s = \pm 1$ is the band index, \mathcal{J}_m is the Bessel function of the first kind of order m and $\epsilon = s\hbar v_F q_\epsilon$ is the energy of the state. Imposing the boundary condition, the allowed energy levels are those in which

$$\frac{\mathcal{J}_{m+1}(q_\epsilon R)}{\mathcal{J}_m(q_\epsilon R)} = s. \quad (27)$$

To apply the polynomial method to this enclosure, we must build the initial functions carefully. The rotation symmetry is continuous:

$$\hat{U}_\phi \Psi = e^{-i(\phi/2)\sigma_z} R_\phi \Psi = \begin{bmatrix} e^{-i\phi/2} \psi_A(r, \theta - \phi) \\ e^{i\phi/2} \psi_B(r, \theta - \phi) \end{bmatrix}.$$

Provided

$$\begin{bmatrix} \psi_A(r, \theta - \phi) \\ \psi_B(r, \theta - \phi) \end{bmatrix} = \begin{bmatrix} e^{-im\theta} \psi_A(r, \theta) \\ e^{-i(m+1)\theta} \psi_B(r, \theta) \end{bmatrix}$$

we get

$$\hat{U}_\phi \Psi = e^{-ik\phi} \Psi, \quad (28)$$

with $k = m + 1/2$. The only functions which are invariant under this symmetry are linear combinations of $|z|^{2n} = r^{2n}$, for $n \geq 0$. For each m , the initial states that respect the symmetries and the BC, $\psi_B/\psi_A = ie^{i\theta}$ are (with $z = x + iy$ and \bar{z} the complex conjugate of z)

$$\begin{aligned} \Psi_0^{(m \geq 0)}(z, \bar{z}) &= z^m \begin{bmatrix} -i \\ z \end{bmatrix}, \\ \Psi_0^{(m < 0)}(z, \bar{z}) &= (\bar{z})^{-(m+1)} \begin{bmatrix} \bar{z} \\ i \end{bmatrix}. \end{aligned} \quad (29)$$

With no loss of generality, we discuss the states with $m = 0$. The procedure is analogous for the remaining representations. A polynomial state can have the form

$$|P(r), Q(r)\rangle = \begin{bmatrix} -iP(r) \\ zQ(r) \end{bmatrix} \quad (30)$$

if P and Q are even polynomials in r such that $P(1) = Q(1) = 1$, thus respecting both the BC and the symmetries in question. Simple monomials $P_n(r) = r^{2n}$ satisfy both conditions and a non-orthogonal basis is

$$\{|P_0, P_0\rangle, |P_1, Q_0\rangle, |P_0, P_1\rangle, |P_2, P_0\rangle, |P_0, P_2\rangle, \dots\} \quad (31)$$

After applying the G-S process, the Hamiltonian is straightforwardly computed and diagonalized for different basis sizes.

The comparison with the exact results is presented in Table 1. As the method quickly converges towards the exact results, we will now apply it to the square enclosure with the same BC.

Basis Size	ϵ_0	ϵ_1	ϵ_2	ϵ_3
2	1.4415	-2.77485		
3	1.4344	-3.20749	4.17305	
5	1.4347	-3.11371	4.61325	-7.05342
7	1.4347	-3.11287	4.67908	-6.30658
Exact	1.4347	-3.11286	4.6801	-6.26629

Table 1: Convergence of polynomial method for the circular enclosure.

3.4 Non-Dirichlet Square Enclosure

The case of square with edges at $x, y = \pm L/2$ and $t = 1$ has no known analytic solution. As these boundary conditions correspond to an uniform gap outside the enclosure, the Hamiltonian will be invariant under $\pi/2$ rotations.

$$\hat{U} = e^{-i\frac{\pi}{4}\sigma_z} R_{\pi/2}$$

The one-dimensional representations of this symmetry are given by

$$\hat{U}\Psi = e^{i\alpha}\Psi,$$

where

$$\alpha = \frac{\pi}{4} + n\frac{\pi}{2} \in [-\pi, \pi]. \quad (32)$$

The other possible symmetries of the Hamiltonian would be reflections. These, however, change the sign of the mass gap outside the enclosure and are also not compatible with the imposed boundary conditions.

The following are low order polynomial functions, belonging to each of the representations of the symmetry group.

$$\begin{aligned} \Phi_{\pi/4} &= \begin{bmatrix} \bar{z} \\ 1 \end{bmatrix}, & \Phi_{-3\pi/4} &= \begin{bmatrix} z \\ z^2 \end{bmatrix}, \\ \Phi_{3\pi/4} &= \begin{bmatrix} \bar{z}^2 \\ \bar{z} \end{bmatrix}, & \Phi_{-\pi/4} &= \begin{bmatrix} 1 \\ z \end{bmatrix}. \end{aligned} \quad (33)$$

Each time we multiply one of these states by $z^m \bar{z}^n$, α changes as

$$\alpha \rightarrow \alpha + (n - m) \frac{\pi}{2}. \quad (34)$$

We stay in the same irreducible representation, provided α is unchanged modulo 2π , *i.e.*, if

$$n - m = 0 \pmod{4}. \quad (35)$$

Invariant monomials of z and \bar{z} are $|z|^2, z^4, (\bar{z})^4$ and their products. There are two issues that need to be addressed at this point:

- (a)** the states of Eq.(33) do not satisfy the BC, and are therefore not suitable as starting states upon which to build a basis. Taking the $\alpha = -\pi/4$ as an example, we require states of the form

$$\Phi_0 = \begin{bmatrix} P_0 \left(|z|^2, z^4, (\bar{z})^4 \right) \\ zQ_0 \left(|z|^2, z^4, (\bar{z})^4 \right) \end{bmatrix} \quad (36)$$

where the invariant polynomials, satisfy $P_0 - Q_0z = 1$ for $y = -1/2$. If this is verified at this edge, the symmetry will ensure the BC are also verified at the other edges. The choice

$$P_0 = -\frac{i}{5} - iz^4 + \frac{i}{5}\bar{z}^4, \quad Q_0 = 1 + \frac{z^4}{5} - 2|z|^2 - \frac{1}{5}\bar{z}^4 \quad (37)$$

proved convenient in the sense that the behaviour of the ket $\Phi_0(x, y)$ near the origin resembles that of the lowest eigenvalue of the circular enclosure,

- (b)** the basis must be built by multiplying each component of the spinor by increasing order invariant polynomials which are required to be unity at the edges of the enclosure so that the BC are preserved. Such polynomials can be generated order by order, by imposing $P_n \left(|z|^2, z^4, (\bar{z})^4 \right) = 1$ for $y = -1/2$.

Once these steps are performed, the calculation proceeds as for the circle, by orthogonalizing the basis and calculating of the Hamiltonian matrix, separately for each of the 4 symmetry representations. The necessary work is halved because the transformation $\sigma_x \mathcal{K}$ (\mathcal{K} is the complex conjugation operator) changes the sign of the Hamiltonian and preserves the BC; the states of the representations with $\alpha = 1/4, 3\pi/4$ can be obtained from those of $\alpha = -1/4, -3\pi/4$ by this transformation; the eigenvalue spectrum remains symmetrical.

The spectrum is displayed in Fig.6, with the low-energy regime in the inset. The number of polynomials in the legend refers to the basis size in each irreducible representation.

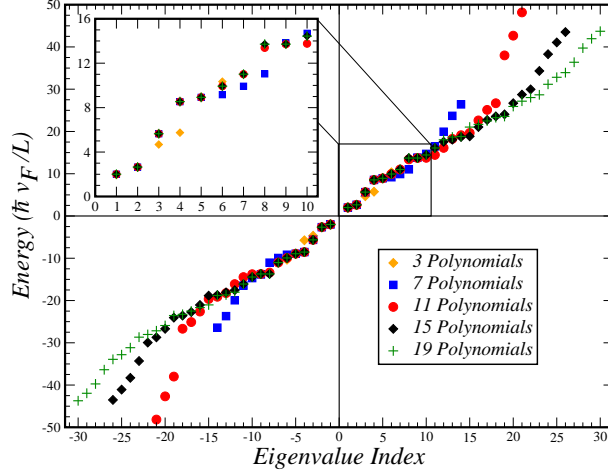


Figure 6: Comparison of the spectrum of the uniform-BCs square billiard with increasing number of polynomials.

This method again converges, as it did in case of the circular enclosure.

As stated before, the method also provides the eigenstates as polynomials. The valence band state with energy closest to zero is plotted in Fig.7. At the center of the square, the behaviour of the two spinor components is not unlike that of the corresponding state of the circle, but is quite different at the edges. The two components have the same absolute value at the edges, as required by the BC, and both vanish at the corners, as that is the only way the BC of the edges that meet at the corner can be satisfied.

To finalize the analysis of the method, we tested it in a problem with BCs analogous to those found in zigzag-terminated hexagonal graphene flakes.

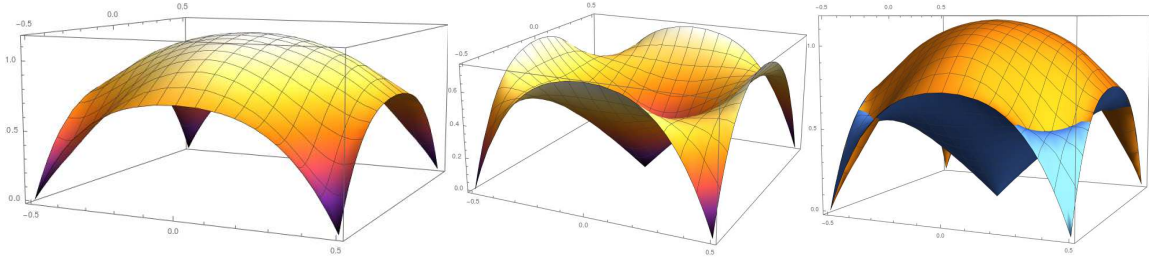


Figure 7: Absolute values of the spinor wave-functions for the eigenstate of energy $\epsilon = -2.0\hbar v_F/L$. Left panel, $|\psi_A|$; middle, $|\psi_B|$; right, both components, showing that $|\psi_A| = |\psi_B|$ at the edges as required by the BC. Near the center of the square the behaviour resembles that of the corresponding state for the circle, but here the spinor wavefunction is zero at the vertexes, as this is the only way to satisfy the BC for the two edges that meet at the vertex (colour online).

3.5 Dirichlet Hexagonal Enclosure

We applied this method to the study of an hexagonal enclosure with the BCs equivalent to those of an hexagonal graphene flake whose edges are all zigzag-terminated. This specific set of BCs can be expressed by alternating t between $t = 0$ and $t \rightarrow \infty$, depending on the termination sublattice.

As we are working with Dirichlet boundaries in alternating sides for each spinor component, we can construct the initial polynomial as in equation 5. Considering a regular hexagon centered at the origin of side-length L , the two spinor components for the starting state will be defined as

$$\begin{aligned} \psi_{0,A}(x,y) &= \left[\frac{\sqrt{3}L}{2} + y \right] \left[L + \left(x - \frac{y}{\sqrt{3}} \right) \right] \\ &\quad \times \left[L - \left(x + \frac{y}{\sqrt{3}} \right) \right] \\ \psi_{0,B}(x,y) &= \psi_A(x, -y). \end{aligned} \quad (38)$$

With this, we diagonalize the Hamiltonian

$$\begin{aligned} \langle \Psi_i | H^\dagger H | \Psi_j \rangle &= \langle \psi_{i,A} | (-\hbar^2 v_F^2 \nabla^2) | \psi_{j,A} \rangle + \\ &\quad + \langle \psi_{i,B} | (-\hbar^2 v_F^2 \nabla^2) | \psi_{j,B} \rangle. \end{aligned} \quad (39)$$

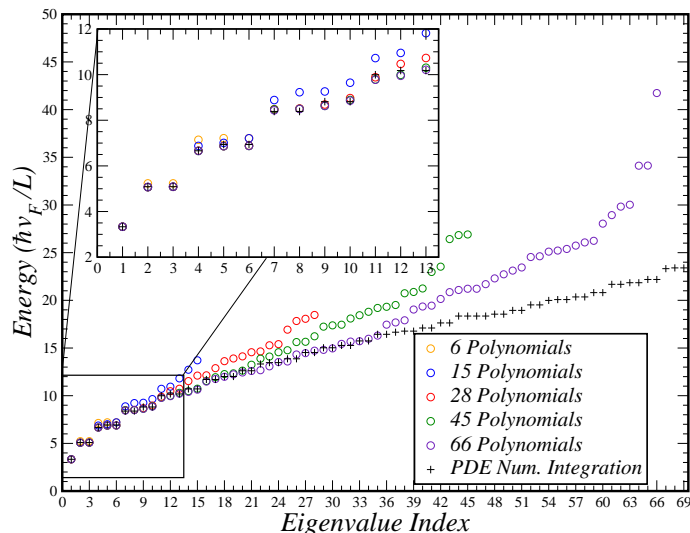


Figure 8: Comparison of the spectrum of the zigzag-like hexagonal enclosure with increasing number of polynomials.

The resulting spectrum is visible in Fig.8 for different basis sizes. The numerical solution was

obtained via *Wolfram Mathematica*[®] by imposing Dirichlet BCs on three alternating sides of the enclosure in question, leaving the remaining free.

Finally, we will compare these results with the ones obtained by Gaddah [14] for the problem of the triangular billiards with boundary condition $\psi_A = 0$ (in our notation, $t \rightarrow \infty$). The exact spectrum described by the author follows the relation (L is the side-length of the equilateral triangle in question)

$$E_{n_1, n_2} = \pm \frac{4}{3} \frac{\pi}{L} \hbar v_F \sqrt{n_1^2 + n_1 n_2 + n_2^2}, \quad (40)$$

where $n_2 \geq n_1 > 0$. As described in the article, the states with $n_2 > n_1$ are (at least) $2\times$ degenerate. The BCs we imposed on a hexagon, $\psi_A = 0$ on three alternating sides (Eq.(38)), also enforce $\psi_A = 0$ on the edges of an equilateral triangle, that contains the hexagon region in question. The condition for ψ_B is the same, as it is a simple inversion of this same triangle. As a consequence, after re-scaling the exact spectrum for the triangle by $\sqrt{A_{\text{hex}}/A_{\text{triang}}}$, we obtain a match between the two as shown in Fig.10. We also compare the density plots for the first three approximate eigenfunctions to those present in Gaddah's work. This comparison (using 10 polynomials) is presented in Fig.9 for $|\psi_A|^2$, with the corresponding regions highlighted.

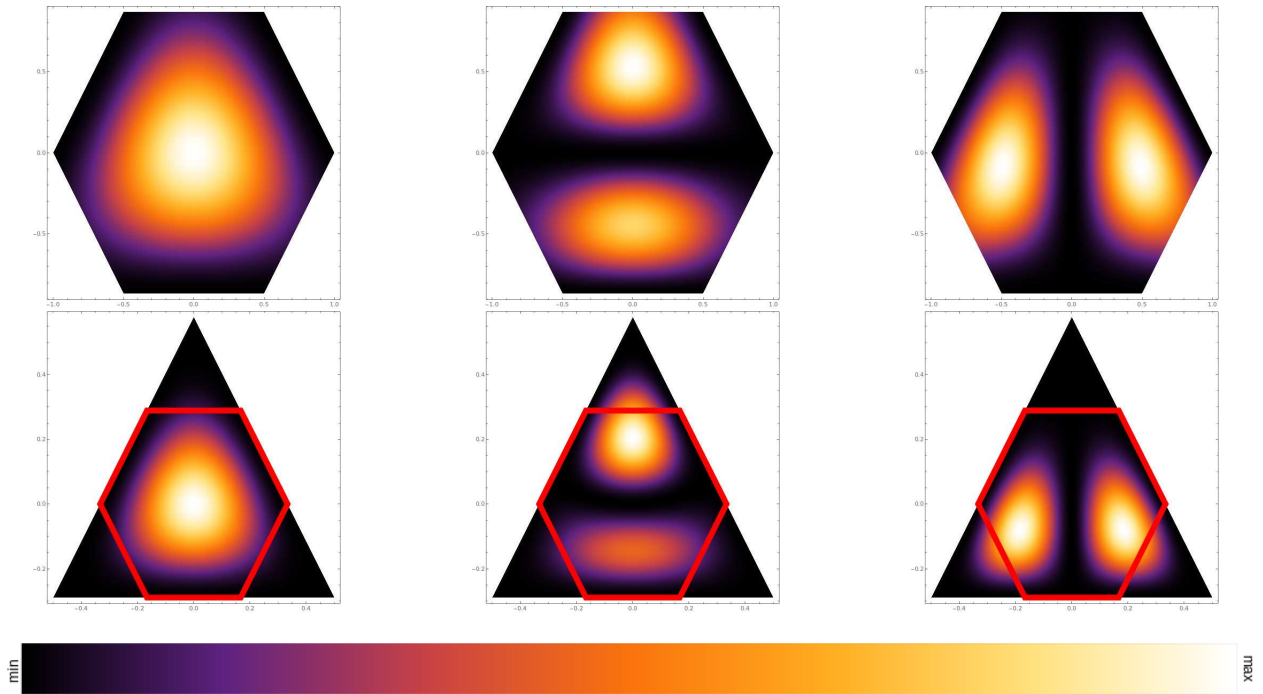


Figure 9: $|\psi_{A,j}|^2$ for the hexagon (top) and for the triangle (bottom) $j \in \{1, 2, 3\}$ (color online).

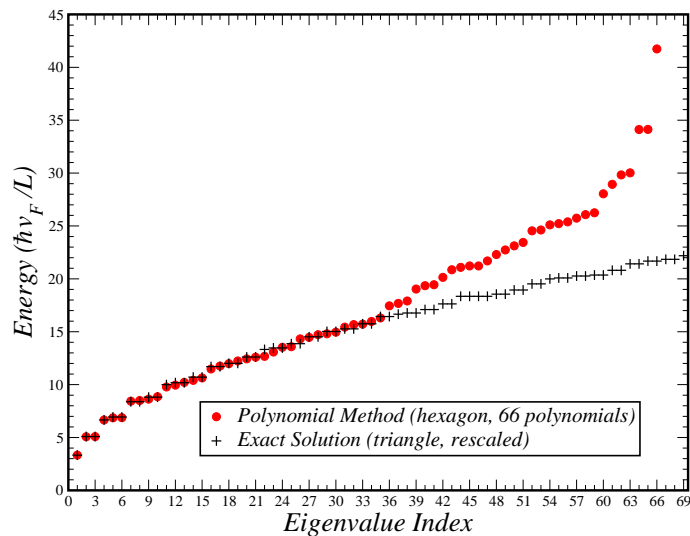


Figure 10: Comparison of the spectrum of the zigzag-like hexagonal billiard against the exact solution for the triangle.

4 Summary and Conclusions

With the polynomial method we have been able to construct approximate solutions to Schrödinger and Dirac-Weyl equations for planar convex polygonal enclosures. The method has been applied before to the determination of frequencies of plate vibrations in the Mechanical Engineering community, but as far as we know its generalization to the Dirac billiards has not been reported before. In this case we considered different types of boundary conditions, including situations where only the ratio of spinors components is specified.

The method is based on constructing a truncated basis of states, all of which satisfy the prescribed BC from the start. By comparing with cases where the exact solution is known (most often by separation of variables) we were able to ascertain the convergence of the method. Typically, a basis size of order $3n$ is required to obtain n eigenvalues with close to 1% accuracy. The method provides not only the lowest energies (or lowest absolute energies for the Dirac -Weyl case) but also eigenstates as finite order polynomials in the coordinates.

Acknowledgments

The authors acknowledge financing of Fundação da Ciência e Tecnologia, of COMPETE 2020 program in FEDER component (European Union), through projects POCI-01-0145-FEDER-028887 and UID/FIS/04650/2019. The authors also acknowledge financial support from Fundação para a Ciência e Tecnologia, Portugal, through national funds, co-financed by COMPETE-FEDER (grant

References

- [1] G. Lamé. Leçons sur la Théorie Mathématique de l'Elasticité. *Bachelier, 1852*.
- [2] M.A. Pinsky. The Eigenvalues of An Equilateral Triangle. *Siam Journal On Mathematical Analysis*, 11(5):819–827, 1980.
- [3] BJ McCartin. Eigenstructure of the equilateral triangle, Part I: The Dirichlet problem. *Siam Review*, 45(2):267–287, JUN 2003.
- [4] V Amar, M Pauri, and A Scotti. Schrödinger-equation For Convex Plane Polygons - A Tiling Method For The Derivation Of Eigenvalues And Eigenfunctions. *Journal of Mathematical Physics*, 32(9):2442–2449, Sep 1991.
- [5] Wai-Kee Li and S. M. Blinder. Particle in an equilateral triangle: Exact solution of a nonseparable problem. *Journal of Chemical Education*, 64(2):130, February 1987.
- [6] W. A. Gaddah. A Lie group approach to the Schrödinger equation for a particle in an equilateral triangular infinite well. *European Journal of Physics*, 34(5):1175–1186, July 2013.
- [7] V Amar, M Pauri, and A Scotti. Schrödinger-equation For Convex Plane Polygons .2. A No-go Theorem For Plane-waves Representation Of Solutions. *Journal Of Mathematical Physics*, 34(8):3343–3350, Aug 1993.
- [8] Berry Michael Victor and Mondragon R. J. Neutrino billiards: time-reversal symmetry-breaking without magnetic fields. *Proceedings of the Royal Society of London. A. Mathematical and Physical Sciences*, 412(1842):53–74, July 1987.
- [9] K. S. Novoselov, A. K. Geim, S. V. Morozov, D. Jiang, M. I. Katsnelson, I. V. Grigorieva, S. V. Dubonos, and A. A. Firsov. Two-dimensional gas of massless Dirac fermions in graphene. *Nature*, 438(7065):197–200, November 2005.
- [10] A. H. Castro Neto, F. Guinea, N. M. R. Peres, K. S. Novoselov, and A. K. Geim. The electronic properties of graphene. *Reviews of Modern Physics*, 81(1):109–162, January 2009.
- [11] L. A. Ponomarenko, F. Schedin, M. I. Katsnelson, R. Yang, E. W. Hill, K. S. Novoselov, and A. K. Geim. Chaotic Dirac Billiard in Graphene Quantum Dots. *Science*, 320(5874):356–358, April 2008.
- [12] Florian Libisch, Christoph Stampfer, and Joachim Burgdörfer. Graphene quantum dots: Beyond a Dirac billiard. *Physical Review B*, 79(11):115423, March 2009.

- [13] M. Zarenia, A. Chaves, G. A. Farias, and F. M. Peeters. Energy levels of triangular and hexagonal graphene quantum dots: a comparative study between the tight-binding and the Dirac approach. *Physical Review B*, 84(24):245403, December 2011.
- [14] W. A. Gaddah. Exact solutions to the Dirac equation for equilateral triangular billiard systems. *Journal of Physics A: Mathematical and Theoretical*, 51(38):385304, September 2018.
- [15] Liang Huang, Ying-Cheng Lai, and Celso Grebogi. Characteristics of level-spacing statistics in chaotic graphene billiards. *CHAOS*, 21(1), MAR 2011.
- [16] Liang Huang and Ying-Cheng Lai. Perspectives on relativistic quantum chaos. *Communications in Theoretical Physics*, 72(4), APR 1 2020.
- [17] Y Shimizu and A Shudo. Polygonal Billiards - Correspondence Between Classical Trajectories And Quantum Eigenstates. *Chaos Solitons & Fractals*, 5(7):1337–1362, Jul 1995.
- [18] R.B. Bhat. Flexural vibration of polygonal plates using characteristic orthogonal polynomials in two variables. *Journal of Sound and Vibration*, 114(1):65–71, January 1987.
- [19] K. M. Liew, K. Y. Lam, and S. T. Chow. Free vibration analysis of rectangular plates using orthogonal plate function. *Computers & Structures*, 34(1):79–85, January 1990.
- [20] K. M. Liew and K. Y. Lam. A Set of Orthogonal Plate Functions for Flexural Vibration of Regular Polygonal Plates. *Journal of Vibration and Acoustics*, 113(2):182–186, April 1991.
- [21] H. Larcher. Notes on orthogonal polynomials in two variables. *Proceedings of the American Mathematical Society*, 10(3):417–423, 1959.
- [22] M. Quintela. From the 1D Schrödinger infinite well to Dirac-Weyl graphene flakes. Master’s thesis, Faculdade de Ciências, Universidade do Porto, 2019.
- [23] B. Wunsch, T. Stauber, and F. Guinea. Electron-electron interactions and charging effects in graphene quantum dots. *Phys. Rev. B*, 77:035316, Jan 2008.

This figure "Sq_eigenstateA.png" is available in "png" format from:

<http://arxiv.org/ps/2007.16176v1>

This figure "Sq_eigenstateAB.png" is available in "png" format from:

<http://arxiv.org/ps/2007.16176v1>

This figure "Sq_eigenstateB.png" is available in "png" format from:

<http://arxiv.org/ps/2007.16176v1>

This figure "cft.png" is available in "png" format from:

<http://arxiv.org/ps/2007.16176v1>